Table 1. Results of N$_2$ adsorption tests for coated
carbon membranes

Micropore volume	0.054 cm^3/g
Characteristic energy of adsorption	21.8 kJ/mol
Specific surface area	1120 m^2/g
Half-width of micropores	0.60 nm

with radii up to 390 nm. No pores with the radii more
than 45 nm (pore size determination limit of the
technique used) were detected in the coated carbon
membranes.

In conclusion, pyrolytic coating of carbon
membranes with TiC and subsequent chlorine treatment
resulted in the formation of a thin microporous carbon
layer on the outer surface of the membranes. Mesopores
of the outer skin of carbon membranes were blocked by
the microporous layer to give an asymmetrical
microporous carbon membrane. The separation
properties of the coated carbon membranes are being
studied.

Institute for Polymer Science   V.M. LINKOV
University of Stellenbosch   R.D. SANDERSON
Stellenbosch 7600
SOUTH AFRICA

Saint Petersburg Technological   G.K. IVAKHNYUK
Institute
Saint Petersburg
RUSSIA

REFERENCES

1. J.E. Koresh and A. Soffer, *Sep. Sci. Technol.*, **18**, 723 (1983).
2. V.M. Linkov, R.D. Sanderson, and E.P. Jacobs, *34th IUPAC Symposium on Macromolecules*, 1992, 7-P56.
3. V.M. Linkov, R.D. Sanderson and E.P. Jacobs, *J. Membr. Sci.*, submitted.
4. J.N. Armor, *ChemTech*, **22**, 557 (1992).
5. J.L. Schmitt, *Carbon*, **29**, 743 (1991).
6. O.E. Babkin, G.K. Ivakhnyuk, and N.F. Fyodorov, *Zhur. Prikl. Khim.*, **3**, 504 (1984).
7. I.N. Ermolenko, I.P. Lyubliner, N.V. Gulko, In *Chemically Modified Carbon Fibers and Their Applications*, VCH, Weinheim (1990), pp. 200-201.
8. Y. Chong and H. Ohara, *J. Fluorine Chem.*, **57**, 169 (1992).

"Harmless" carbon tubes around "dangerous" asbestos fibres

Carbon nanotubes were found first by Iijima in soot-like
deposits on the cathode of a carbon-arc chamber [1].
Their formation is based on graphitic planes rolling up at
high temperatures to form seamless cylinders [1,2,3].
Following the principles of capillary suction of the
carbon tubes [4], a Pb-containing phase as well as
yttrium carbide have been successfully introduced inside
pre-existing carbon tubes [5,6]. We have, for the first
time, demonstrated that the growth of carbon tubes can
take place around asbestos fibres (Mg$_3$Si$_2$O$_5$(OH)$_4$).
The asbestos cylinders behave as substrates around
which the nucleation and growth of carbon tubes take
place.

A small amount of asbestos fibres, with a
diameter between 20 and 40 nm, was mixed into the arc
chamber during the preparation of the carbon tubes. A
carbon soot bar deposited on the cathode was broken and
soot pieces were scraped out from the broken section.
By means of scanning electron microscopy, the asbestos
needles were located. A number of carbon nano-tubes
and needles were picked up, crushed and suspended on a
holey carbon copper grid for examination in a 200kV
transmission electron microscope.

Fig. 1a shows several individual cylindrical
asbestos fibres encapsulated by carbon tubes. The
cylindrical asbestos (black) inside the carbon tubes are
found to be either hollow or solid, in agreement with the
observation of Yada [7]. Selected-area electron
diffraction (SAED) patterns demonstrate the well
crystallined cylindrical asbestos structure which we will
describe later. Most encapsulated asbestos fibres are
straight, but sinusoidal and curved morphologies are also
present (indicated by arrows A,B,C and D), particularly
in some relatively short carbon tubes. This sinusoidal
morphology is particularly visible in fig. 1b. The tubes
surrounding the asbestos fibres vary from 0.1 μm to
more than 1μm in length, while the diameters are
between 20 nm and 50 nm. The majority of the tubes
however have diameters around 30-40 nm, which is
substantially larger than that for pure carbon nanotubes
[8,9]. The thickness of the tube wall is about 3 nm.
Tilting around the length axis of the tube does not alter
its shape, confirming the cylindrical shape of the tube.
Some of the tubes however have a prismatic shape,
which is evidenced by tilting the tube around the cylinder
axis. Most of tubes are closed at both ends with dome
caps (arrows A and B) though opened ends are not
exceptional (arrows C and D). The opened ends
however can be a consequence of crushing and breaking
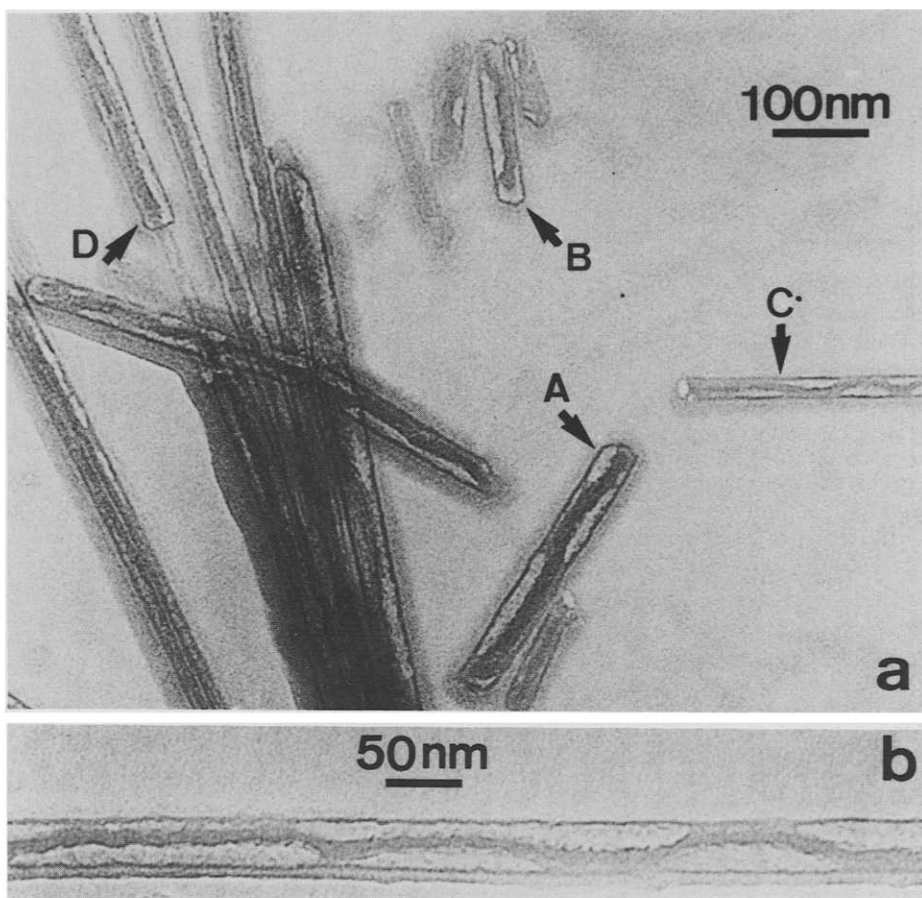the sample during preparation for transmission electron

Fig. 1. (a) Morphology of the carbon tubes surrounding asbestic fibres. Arrows A, B, C and D indicate tubes with sinusoidally shaped asbestos inside. Tubes indicated by arrows A and B are closed at both ends whereas those indicated by arrows C and D have open ends. (b) Part of tube C at a larger magnification. The sinusoidal shape of the encapsulated asbestos fibre is clearly visible. The assymetrical projecting tube shape (double edge lines in the bottom and single in the top) suggests a prismatic shape of the tube.

microscopy. The empty or amorphous regions between the asbestos fibre and encapsulating tube may be due to a chemical reaction of asbestos with the carbon tubes. This reaction could explain the rough surface of the asbestos fibres as presented in fig 1. Moreover, attempts to obtain lattice images of the carbon tubes or of the asbestos fibres failed because of the fast amorphous transition under the electron beam.

Energy-dispersive X-ray spectroscopy (EDX) was performed to investigate the tube content. The regions used to obtain the spectra are carefully selected and marked in fig. 2 by A and B. Region A comprises a part of interior asbestos and the surrounding tube whereas region B comprises only part of the surrounding tube. The spectra recorded from regions A and B are depicted in fig. 3a and fig. 3b, respectively. Mg, Si, O and C peaks in fig. 3a are consistent with the $Mg_3Si_2O_5(OH)_4$ composition of the asbestos fibre. The fact that the Mg peak disappears while the Si and O peaks are strongly weakened in region B, confirms that the outer surrounding tubes are not asbestos-related; the surrounding tubes only consist of carbon. The remaining Cu-peak is due to the copper support grid. We have convinced ourselves that the tubes are not formed under the electron beam, and we have also verified that the tubes are not to be confused with specimen contamination.
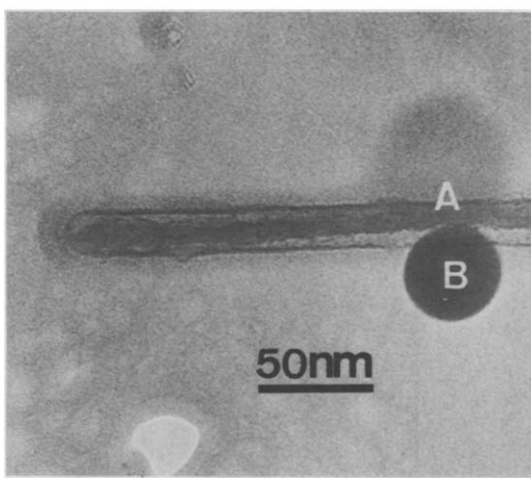

Fig. 2. A tube with asbestos used for EDX analysis. Two circular dark regions are caused by electron beam contamination during the spectra acquisition. Region A contains a part of interior asbestos as well as the surrounding carbon tube; region B only contains a part of the carbon tube.
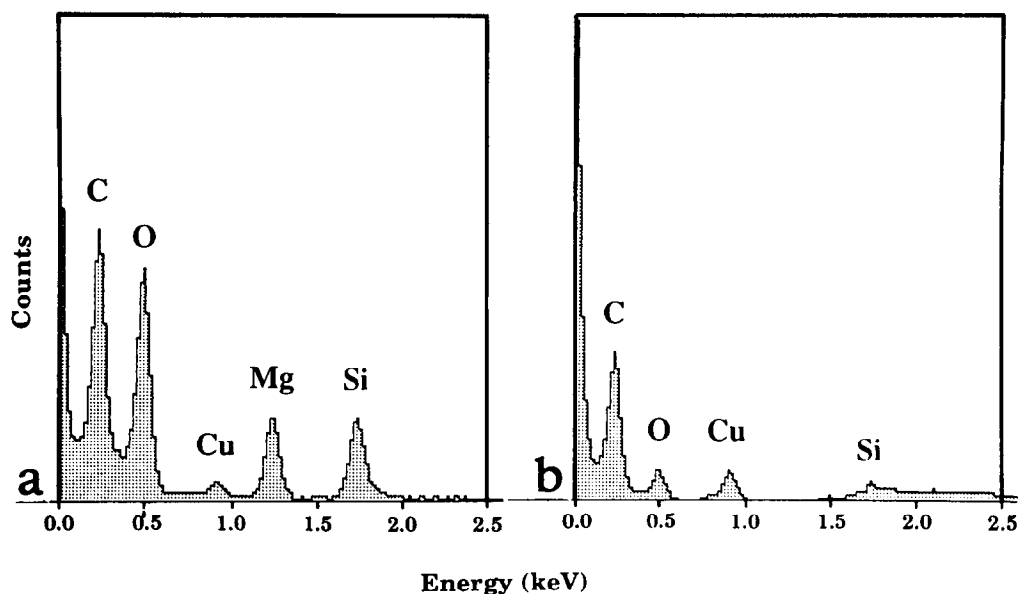
Fig. 3. EDX spectra from (a), region A and (b), region B in fig. 2.

Selected-area electron diffraction (SAED) patterns obtained from individual asbestos fibres inside the carbon tube are shown in fig. 4. The pattern of fig. 4a is symmetrical with respect to the vertical axis, which is typical for a cylindrical wrapping of the crystal structure and has also been observed for the pure carbon tubes [2,3]. The present pattern can be perfectly indexed according to the monoclinic structure of asbestos [10], taking into account the cylindrical symmetry of the fibre, which introduces apparent twin related patterns, as the ones indicated in fig. 4a by full and broken lines. The

reciprocal angle $\beta' = 87°$ corresponds to the monoclinic angle $\beta = 93°$ in real space. The simultaneous appearance of (h00), (0k0) and (00l) reflection rows in one SAED pattern is a typical and well known feature for cylindrical structures [2,3]. The unique rolling direction as well as the non-helical feature of the asbestic cylinders can be concluded from the fact that no SAED patterns differing from the one in fig. 4a have been found. As pointed out by Pauling, the asymmetrical layered structure of asbestos is perfectly suited to form the cylindrical shape [11].
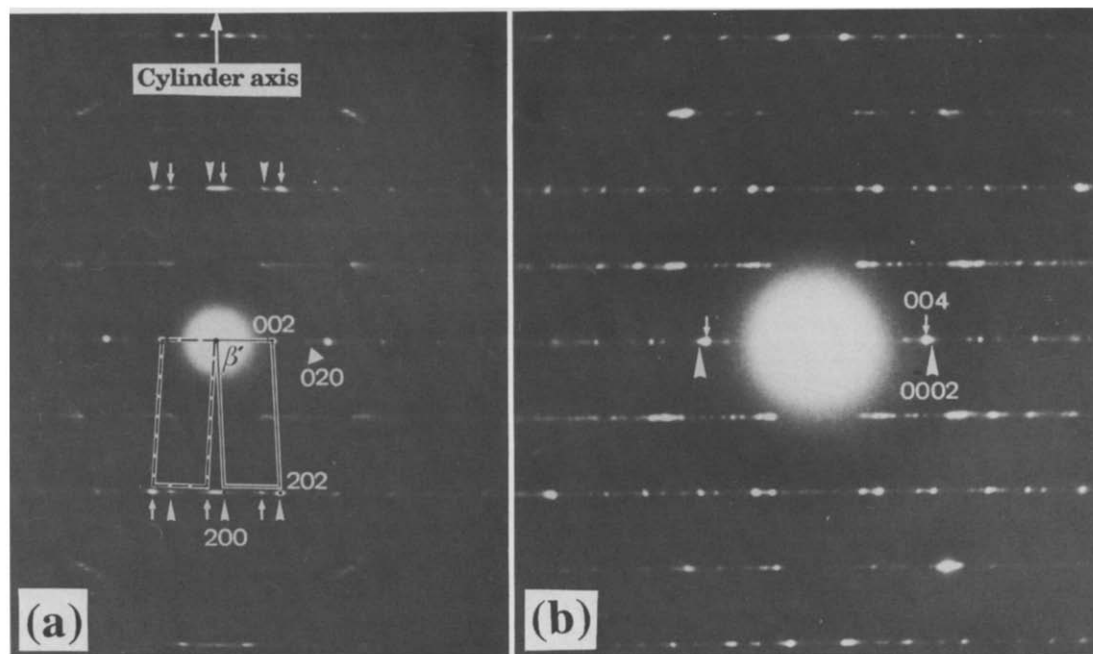

Fig. 4. (a) SAED pattern from an asbestos and carbon tube entity. The reflections are indexed according to the monoclinic $Mg_3Si_2O_5(OH)_4$. Two parallellograms which locate symmetrically with respect to the cylinder axis are outlined by full and broken lines. Reflections arising from two regions of the asbestos fibre are indicated by small arrowheads and arrows respectively. (b) SAED pattern showing the presence of the (0002) graphite reflection next to the (004) asbestos reflection.

In fresh samples and by careful selection, the representative (0002)-type reflections of the tubular graphite structure can be discerned in the SAED patterns (fig. 4b). These reflections, which correspond to a 3.45Å lattice spacing in real space, are lying very close to the asbestos (004) reflection but can still be distinguished as indicated by arrowheads in fig. 4b. Presumably, they imply a graphite structure for the tubes surrounding the asbestos fibres, though we have not yet obtained sufficient evidence for the graphite structure. Contrary to the empty tubes, or to pure graphite, the present surrounding carbon tubes easily disintegrate; most probably because of the unstable behavior of asbestos under the electron beam [7].

A possible growth model for the carbon tubes around the asbestos fibres is based on the idea that the asbestos fibres behave as substrates for carbon growth. Carbon tubes probably nucleate randomly and grow independently along the asbestos fibre. These independently grown tubes finally coalesce to form the complete tubes as observed in fig. 1. The whole procedure is schematically illustrated in fig. 5. It is reasonable to assume, as shown in fig. 5a, that the nucleations prefer to start at both ends of the asbestos substrate though nucleations at other places are possible. These separate nucleations grow independently along the asbestos fibre by continuously adding carbon atoms (fig. 5b). When two tube pieces meet (fig. 5c), two situations may occur which are illustrated either in fig. 5d or in fig. 5e. For the former situation, the coalescence is perfect, and the length of the tube will be the same as the length of the encapsulated asbestos fibre, which keeps its

original (straight) shape. However, in a number of situations the connections between adjacent tube pieces will not be perfect and strains will be generated at the interconnections. The strain along the cylinder axis can be relaxed by altering the tube length. In the case of a length reduction, the interior asbestos will be forced to bend within the diminished space as shown in fig. 5e. Both situations represented schematically in fig. 5d and fig. 5e are indeed observed in fig. 1a.

If we would on the contrary suppose that the carbon tubes nucleate and grow along an originally sinusoidal shaped asbestos fibre, sinusoidal carbon tubes should result. This however has never been observed; the surrounding carbon tubes are always straight, independent of whether the interior asbestos is straight or sinusoidal. In addition, no half or partially filled tubes have been observed. These facts are convincing evidence that carbon tubes nucleate and grow around the pre-existing asbestos fibres.

The present results illustrate for the first time the possibility of growing a "harmless" carbon protection around microscopic fibres, which could be toxic or chemically active. We are indeed convinced that asbestos fibres are not the only fibres which can be wrapped in a carbon protection; experiments on other fibre-like materials are under the way.
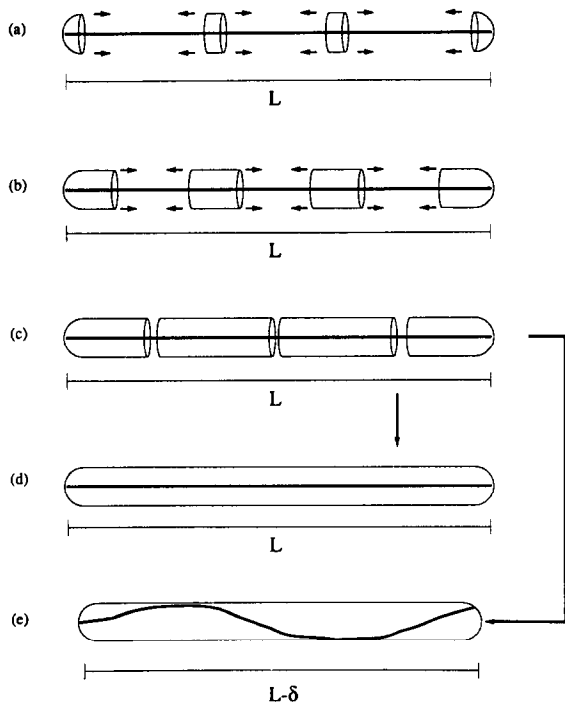
Fig. 5. Illustration of a possible growth procedure of carbon tubes around the asbestos fibre. (a) Nucleation of carbon tubes along the asbestos. (b) Continued growth of tube pieces. (c) Individual tube pieces are going to coalesce. (d) Final tube of length L is formed in the case of a perfect connection between tube pieces. (e) Final tube with a shortened length L - δ is formed in the case of strain connections between the tube pieces. The interior asbestos will be bent in this case.

EMAT, Univ. of Antwerp (RUCA)   X.F. ZHANG*
Groenenborgerlaan 171   X.B. ZHANG†
B-2020 Antwerp   G. VAN TENDELOO
BELGIUM

Research Institute of Materials   G. MEIJER
University of Nijmegen
6525 ED Nijmegen
THE NETHERLANDS

*On leave from Beijing Laboratory of Electron Microscopy, Chinese Academy of Sciences, China.
†On leave from Zhejiang Univ., Hangzhou, China

REFERENCES

1. S. Iijima, Nature, 354, 56 (1991).
2. X.F. Zhang, X.B. Zhang, G. Van Tendeloo, S. Amelinckx, M. Op de Beeck and J. Van Landuyt, J. Crystal Growth, 130, 368 (1993).
3. X.B. Zhang, X.F. Zhang, S. Amelinckx, G. Van Tendeloo and J. Van Landuyt, Ultramicroscopy (in press).
4. M.R. Pederson, J.Q. Broughton, Phys. Rev. Lett., 69, 2689 (1992).
5. P.M. Ajayan and S. Iijima, Nature, 361, 333 (1993).
6. S. Seraphin, D. Zhou, J. Jiao, J.C. Withers and R. Loutfy, Nature, 362, 503 (1993).
7. K. Yada, Acta Cryst., 23, 704 (1967).
8. P.M. Ajayan and S. Iijima, Nature, 358, 23 (1992).
9. S. Iijima and T. Ichihashi, Nature, 363, 603 (1993).
10. E.J. Whittaker and J. Zussman, Miner. Mag., 31, 117 (1956).
11. L. Pauling, Proc. Natn. Acad. Sci. U.S.A., 16, 578 (1930).